Publication IV

I. Aaltio, K. P. Mohanchandra, O. Heczko, M. Lahelin, Y. Ge, G. P. Carman, O. Söderberg, B. Löfgren, J. Seppälä, S-P. Hannula. Temperature dependence of mechanical damping in Ni-Mn-Ga austenite and non-modulated martensite. *Scripta Materialia*, 59, pp. 550-553, Doi: 10.1016/j.scriptamat.2008.05.005, May 2008.

ELSEVIER

Scripta MATERIALIA

Temperature dependence of mechanical damping in Ni–Mn–Ga austenite and non-modulated martensite

I. Aaltio,[a,*] K.P. Mohanchandra,[b] O. Heczko,[a,d] M. Lahelin,[c] Y. Ge,[a] G.P. Carman,[b] O. Söderberg,[a] B. Löfgren,[c] J. Seppälä[c] and S.-P. Hannula[a]

[a]*Department of Materials Science and Engineering, Helsinki University of Technology, P.O. Box 6200, FI 02015 TKK, Finland*
[b]*University of California Los Angeles (UCLA), Mechanical and Aerospace Engineering Department,*
Active Materials Laboratory, CA, USA
[c]*Department of Biotechnology and Chemical Technology, Helsinki University of Technology, P.O. Box 6100, FI 02015 TKK, Finland*
[d]*IFW Dresden, Helmholtzstrasse 20, 01069 Dresden, Germany*

The temperature dependence of damping properties of the $Ni_{52.3}Mn_{27.4}Ga_{20.3}$ alloy was studied in the temperature range of 308–473 K. The vibration damping capability of this 2M martensite structure increases above a certain stress level, corresponding well to the twinning stress values observed previously. This triggering stress decreases with increasing temperature. The dominant damping mechanism of the martensitic phase is related to the twin boundary movement. In the martensite–austenite two phase region, $\tan\delta$ decreases above a maximum stress value.
© 2008 Acta Materialia Inc. Published by Elsevier Ltd. All rights reserved.

Keywords: Ni–Mn–Ga; Twin boundary movement; Damping; Martensite

Effective vibration damping capacity, i.e. the property related to the dissipation of mechanical vibration energy, in shape memory alloys (SMAs) is obtained by the dissipative motion of the different phase and twin boundaries [1–3]. In addition to the material properties, the mode of the external vibration and its frequency, waveform and amplitude, external temperature, external loads, possible thermal gradient, etc. have an effect on the damping capacity. Ni–Mn–Ga alloys usually exhibit a thermal shape memory effect (SME) and form stress-induced martensite just above the reverse transformation region. If the martensite crystal structure is of the right type, alloys can show a magnetic shape memory effect (MSME) and magnetically assisted superelasticity (MFAS) [4]. Dynamic mechanical analysis (DMA) was applied mainly to study the transformation behavior of these materials [5–8], but only few results exist of the damping behavior [3,9–11].

Damping capacity can be evaluated based on the value of the loss tangent ($\tan\delta$), which is the phase differ-ence between the applied sinusoidal stress and the resulting strain. For single crystalline Ni–Mn–Ga alloys at room temperature, $\tan\delta$ is found to increase with maximum strain [11], and is dependent on the number of loading cycles [5,9,10]. Under quasi-static mechanical testing with tensile and compressive loading, polycrystalline $Ni_{51}Mn_{28}Ga_{19}$ had a $\tan\delta$ value of 0.4925 [9]. The internal friction (Q^{-1}) method has also been used to determine damping properties of Ni–Mn–Ga [12]. In these studies the vibration amplitudes were small ($\varepsilon_{max} \approx 10^{-4}$) and, in comparison to DMA measurements, relatively small room temperature values, i.e. $Q^{-1} \approx 0.002$ for $Ni_{54.5}Mn_{21.5}Ga_{24.0}$ and $Q^{-1} \approx 0.008$ for $Ni_{52.1}Mn_{27.3}Ga_{20.6}$, were obtained. When comparing the Q^{-1} and $\tan\delta$ values, for relatively small values (e.g. $\tan\delta < 0.1$), the relation $Q^{-1} \approx \tan\delta$ can be used [13]. Damping of $Ni_{52}Mn_{24}Ga_{24}$ single crystal has been shown to depend on the magnetic field applied, especially below the M_s temperature. This has been proposed to originate from the irreversible motion of the martensitic domains, coupled to magnetic domains [11]. In addition, time-dependent twin stabilization (i.e. aging) resulting in logarithmically increasing damping with time has been reported for $Ni_{48.2}Mn_{29.5}Ga_{22.3}$

single crystal [14]. Damping depends also on the external temperature and softening of the material is observed close to the martensitic transformation temperature [6,15]. At higher temperatures Ni Mn Ga alloys have the cubic Heusler structure ($L2_1$), while at lower temperatures these materials may exhibit several martensitic crystal structures, of which the non-modulated 2M structure (also abbreviated as T or NM) is studied here. It has been previously shown that the twinning stress (σ_{tw}) needed for the motion of the twin boundaries can be decreased to nearly 10 MPa at room temperature by cycling, following an increase in temperature to 375 K, can be decreased further to about 8.5 MPa [16]. In the present paper the temperature dependence of the damping behavior of the 2M structure is reported and the damping mechanism discussed.

The studied $Ni_{52.3}Mn_{27.4}Ga_{20.3}$ material was supplied by AdaptaMat Ltd. The ingot was annealed at 1253 K for 48 h and at 1073 K for 72 h in a vacuum quartz ampoule. Single crystal specimens ($10 \times 1.3 \times 35$ mm^3) were cut with EDM, wet ground to 1200 mesh and electropolished in 25% nitric acid ethanol solution. The chemical composition was determined energy-dispersive spectroscopy using an LEO-1450 scanning electron microscope. The crystal structure and orientation were measured at ambient temperature with a Philips X'Pert X-ray diffractometer using Co K_α radiation. The martensite crystal structure was confirmed as 2M by single crystal diffraction. Specimens were cut from the ingot in a suitable direction to obtain necessary dimensions. The sticks were not oriented along the crystallographic axes, but the wider longitudinal sample surfaces (i.e. the flat faces, which were also used in attaching the samples for the DMA measurement) deviated by about 14° from the (0 0 1) plane, and the longitudinal axis of the sample deviated by about 29° from the [1 0 0] direction, both referring to the 2M martensite phase system. These measurements were conducted from the samples after the DMA tests, and X-ray diffraction measurements were made from the flat face of the sample. The structural transformation temperatures and the magnetic transition temperatures were measured using a low-field AC magnetic susceptibility measurement and a Shimadzu SC-50 differential scanning calorimeter (DSC). The characteristic temperatures were found to be as follows: M_s 406 K, M_f 394 K, A_s 409 K, A_f 420 K and T_c 373 K. In the DSC measurements, the rate of temperature change was 8 K min^{-1}.

Damping properties of the alloy were studied using DMA Q800 equipment from TA Instruments. Single cantilever mode and sinusoidally alternating bending stress with a constant 95 Hz frequency and increasing stress amplitude σ_a was applied in an essentially zero magnetic field (i.e. the earth field). Before testing it was confirmed by a low-force frequency sweep at 313 K that the chosen frequency did not coincide with a harmonic frequency of the sample, in order to avoid the influence of the shape of the samples. The measurement frequency was selected to be 95 Hz since it is the dynamic damping behavior of these materials in this range that is of interest in many practical applications. The direction of loading was normal to the flat faces of the sample. The experiments were done with the sam-

ple originally in the multivariant state. The maximum stress and strain amplitudes, corresponding to the values at the sample surfaces, were given by the DMA system.

The DSC measurements indicating martensite to austenite transformation are shown in Figure 1. The figure also indicates the temperatures close to transformation in which the loss tangent, $\tan\delta$, was measured. The onset of the transformation from martensite to austenite occurs at 409 K. The results of the damping measurements, i.e. $\tan\delta$ as a function of stress, are collected in Figure 2a c for the different temperature regions. A clear temperature dependence of the damping behavior is observed when the material is fully martensitic and it has a non-modulated tetragonal structure (Fig. 2a). At lower temperatures (308 and 323 K) straining with all σ_a values remains in the region of 0.1% and the maximum $\tan\delta$ is below 0.27. However, the dependence of the strain on stress is not linear, suggesting the contribution of the twin boundary motion. A significant change in behavior is observed at 348 K, where $\tan\delta$ starts to increase strongly from 0.06 at 11 MPa, until the maximum value of 0.37 at 42 MPa is reached. At 373 K, the more intense damping shown by the strongly increasing $\tan\delta$ starts at 8 MPa, reaching the maximum $\tan\delta$ 0.498 at 42 MPa. This maximum is obtained with the highest stress amplitude obtainable with the applied DMA system. The observed stress onset of the enhanced damping correlates well with the minimum twinning stress (σ_{tw}) values obtained in Ref. [16] after tensile compressive cycling of the non-modulated structure at high temperatures, where the σ_{tw} was about 8.5 MPa at 373 K. During the tensile compressive cycling, the twinning stress, σ_{tw}, decreased after first cycles to approximately 10 MPa at room temperature and to about 8.5 MPa at 373 K. Therefore, it is reasonable to assume that the observed enhanced damping behavior in the non-modulated martensite structure is a result of the twin boundary movement.

Figure 2b shows the damping behavior of martensite close to the transformation temperature to austenite. When the temperature approaches the phase transformation region (Fig. 1) enhanced damping starts with an even lower stress, i.e. 7 MPa. Damping and straining show a sudden increase at about 35 MPa. It is proposed that this is related to the formation of a resonance (i.e.
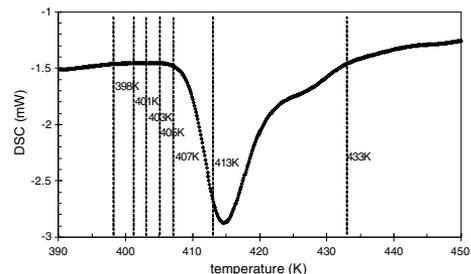

Figure 1. DSC graph showing the martensite to austenite transformation behavior. The $\tan\delta$ (DMA) measurement temperatures, which are close to the transformation temperatures, are indicated by vertical lines.
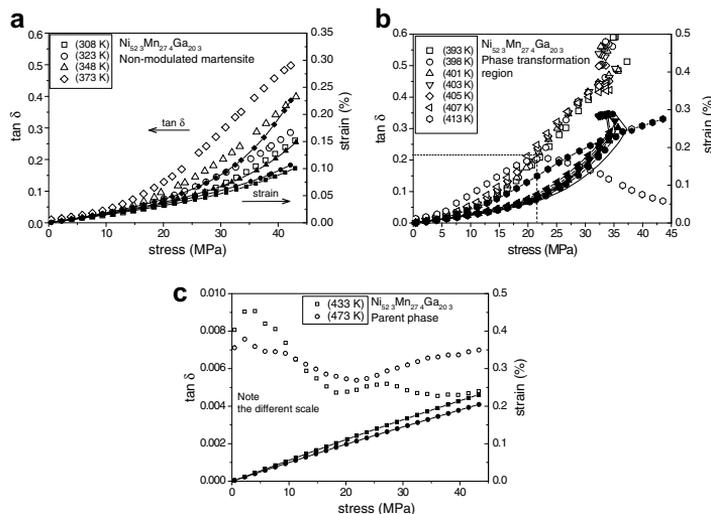
Figure 2. Tan δ (open points) and maximum measured strain (filled points connected by a line) as a function of maximum bending stress (MPa) at different temperatures (K), as marked in the figures. Frequency of the single cantilever mode cycling in the measurements is 95 Hz. (a) Temperature region for the non modulated martensite phase. (b) Phase transformation region. (c) Temperature region for the parent phase.

standing wave) in the martensitic sample that is softened just before the start of the phase transformation [3] in such a way that the previously established harmonic frequency values do not apply any more. In this case, the maximum tan δ at 393 K is 0.59 and at 407 K is 0.42 at a stress level of 34 MPa. Figure 2c shows that the damping capacity of the austenite is very low, in accordance with the results in Refs. [3,6,8], and it is about constant in the stress and temperature ranges measured. In that stress range the materials behave elastically. When the amount of martensite phase decreases above A_s (Fig. 1), a new type of restriction for maximum damping appears (Fig. 2b). The increasing amount of parent cubic austenite phase decreases the damping capability of the material due to the very low damping of the austenite phase. This is indicated at 413 K (Fig. 2b), where the damping increases from a triggering stress of about 7 MPa, similar to that in the fully martensitic structure. However, above 23 MPa (tan δ 0.21) damping starts to decrease again. Here, the increasing stress may result in a situation, where the damping mechanism gradually converts from twin boundary motion to phase boundary movement between the fully oriented martensite and the parent phase.

The stress dependence of dynamic modulus determined from the DMA measurements at different temperatures are shown in Figure 3. In the 2M martensite phase the modulus decreases monotonously with both increasing stress and increasing temperature. The decrease of the modulus with stress may indicate twin boundary motion, which leads to apparent modulus softening. The sharp drop in the modulus with increasing stress at 413 K correlates well with the decrease in damping capacity and can be related to reverse transformation to austenite. In cubic austenite the dynamic
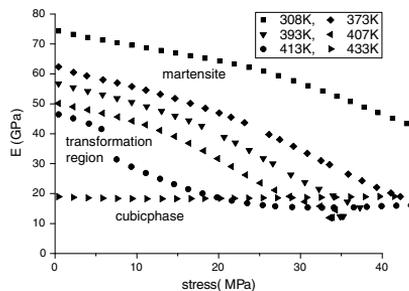

Figure 3. Dynamic modulus E as a function of the bending stress amplitude below, in and above the phase transformation temperature range.

modulus is lower than in martensite and stays more or less constant at about 20 GPa.

The damping behavior of the $Ni_{52.3}Mn_{27.4}Ga_{20.3}$ alloy was established with cantilever DMA measurements for the non-modulated (2M) martensite phase both in the two-phase transition region and in the parent phase. In the martensite the twin boundary motion is suggested to be the main damping mechanism, as damping is clearly enhanced when the applied stress exceeds the twinning stress of the material. Rising temperature decreases this triggering stress for enhanced damping and improves the damping capability, in accordance with previous observations on the increased twin boundary mobility. The maximum observed tan δ value was 0.498 at 373 K at a stress of 42 MPa. In the two-phase region the parent phase restricts the damping, and the damping capacity of austenite is about two orders of magnitude lower.

[1] D.D.L. Chung, J. Mater. Sci. 36 (2001) 5733.
[2] J.V. Humbeeck, S. Kustov, Smart Mater. Struct. 14 (2005) S171.
[3] I. Aaltio, M. Lahelin, O. Söderberg, O. Heczko, B. Löfgren, Y. Ge, J. Seppälä, S. P. Hannula, Mater. Sci. Eng. A 481 482 (2008) 314.
[4] O. Söderberg, I. Aaltio, Y. Ge, O. Heczko, S. P. Hannula, Mater. Sci. Eng. A 481 482 (2008) 80.
[5] E. Césari, V.A. Chernenko, V.V. Kokorin, J. Pons, C. Seguí, Acta Mater. 45 (1997) 999.
[6] C. Seguí, E. Césari, J. Pons, V. Chernenko, Mater. Sci. Eng. A 370 (2004) 481.
[7] C. Seguí, E. Césari, J. Font, J. Muntasell, V.A. Chernenko, Scripta Mater. 53 (2005) 315.
[8] C. Seguí, V.A. Chernenko, J. Pons, E. Césari, V. Khovailo, T. Takagi, Acta Mater. 53 (2005) 111.
[9] D.A. Ruggles, E. Gans, K.P. Mohanchandra, G.P. Carman, E. Ngo, W. Nothwang, M.W. Cole, Proc. SPIE 5387 (2004) 156.
[10] E. Gans, C. Henry, G. Carman, Proc. SPIE 5387 (2004) 177.
[11] W.H. Wang, G.D. Liu, G.H. Wu, Appl. Phys. Lett. 89 (2006) 101911.
[12] V.G. Gavriljuk, O. Söderberg, V.V. Bliznuk, N.I. Gla vatska, V.K. Lindroos, Scripta Mater. 49 (2003) 803.
[13] J. Graesser, C.R. Wong, in: V.K. Kinra, A. Wolfenden (Eds.), M^{3}D: Mechanics and Mechanisms of Material Damping, vol. 1169, ASTM STP, 1992, p. 316.
[14] L. Dai, M. Wuttig, E. Pagounis, Scripta Mater. 55 (2006) 807.
[15] C. Seguí, V.A. Chernenko, J. Pons, E. Césari, V. Khovailo, T. Takagi, Acta Mater. 53 (2005) 111.
[16] O. Söderberg, L. Straka, V. Novák, O. Heczko, S. P. Hannula, V.K. Lindroos, Mater. Sci. Eng. A 386 (2004) 27.